Samantha M. Desmarais[1]
Thomas Leitner[2]
Annelise E. Barron[1]*

[1]Department of Bioengineering, Stanford University, Stanford, CA, USA
[2]Los Alamos National Laboratory, Theoretical Biology and Biophysics, Los Alamos, NM, USA

Received August 16, 2011
Revised October 12, 2011
Accepted October 13, 2011

Research Article

Quantitative experimental determination of primer–dimer formation risk by free-solution conjugate electrophoresis

DNA barcodes are short, unique ssDNA primers that ''mark'' individual biomolecules. To gain better understanding of biophysical parameters constraining primer–dimer formation between primers that incorporate barcode sequences, we have developed a capillary electrophoresis method that utilizes drag-tag-DNA conjugates to quantify dimerization risk between primer-barcode pairs. Results obtained with this unique free-solution conjugate electrophoresis approach are useful as quantitatively precise input data to parameterize computation models of dimerization risk. A set of fluorescently labeled, model primer-barcode conjugates were designed with complementary regions of differing lengths to quantify heterodimerization as a function of temperature. Primer–dimer cases comprised two 30-mer primers, one of which was covalently conjugated to a lab-made, chemically synthesized poly-*N*-methoxyethylglycine drag-tag, which reduced electrophoretic mobility of ssDNA to distinguish it from ds primer–dimers. The drag-tags also provided a shift in mobility for the dsDNA species, which allowed us to quantitate primer–dimer formation. In the experimental studies, pairs of oligonucleotide primer barcodes with fully or partially complementary sequences were annealed, and then separated by free-solution conjugate CE at different temperatures, to assess effects on primer–dimer formation. When less than 30 out of 30 base-pairs were bonded, dimerization was inversely correlated to temperature. Dimerization occurred when more than 15 consecutive base-pairs formed, yet non-consecutive base-pairs did not create stable dimers even when 20 out of 30 possible base-pairs bonded. The use of free-solution electrophoresis in combination with a peptoid drag-tag and different fluorophores enabled precise separation of short DNA fragments to establish a new mobility shift assay for detection of primer–dimer formation.

Keywords:
CE / Dimerization / DNA barcodes / Drag-tag / Mobility shift assay
DOI 10.1002/elps.201100452

1 Introduction

DNA barcodes are short, unique ssDNA primers that are appended to individual biomacromolecules, and are required by numerous methods for DNA and protein detection. Barcodes are an essential component of multiplexing, which is the simultaneous measurement of multiple analytes in a single sample. Inherent in the challenge to create well-designed barcodes is that the more multiplexing required, the more barcodes that are needed and the harder it is to design a unique barcode. Multiplexing is widely used across all areas of science, in methods such as PCR for applications requiring the amplification or sequencing of DNA (such as 454™ sequencing and STR analysis) [1–4] and biomarker analysis for different diseases [5–7]. In the case of 454™ sequencing, multiplexed samples identified by DNA oligomer barcodes can lead to an amplification bias that occurs through creation of libraries for purification, amplification and sequencing, preventing good sequencing results [8]. With constraints imposed on nucleotide content by elements such as 454™-adaptors, specific PCR primers

Correspondence: Dr. Samantha Desmarais, Department of Bioengineering, Stanford University, 318 Campus Drive, Stanford, CA 94305-5444, USA
E-mail: sdesmar@stanford.edu
Fax: +1-650-723-9801

Abbreviations: FSCE, free-solution conjugate electrophoresis; **NMEG,** *N*-methoxyethylglycine

*Additional corresponding author: Dr. Annelise Barron
E-mail: aebarron@stanford.edu

Colour Online: See the article online to view Figs. 2–5 in colour.

for amplification and unique barcode tags to be incorporated into the final primer design [2], the risk of primer-dimerization is high when multiplexing with 454™ sequencing. Although DNA hybridization has been utilized in approaches such as PCR [9, 10], dimer-based molecular probes [11], and sequencing [2], determination of factors influencing primer–dimer formation has not been specifically studied. Dimerization risk and melting temperatures of primer barcodes must be considered and weighed appropriately to predict useful primer barcodes.

A range of methods have been applied to analyze different conformations of DNA. The most common are solid-phase hybridization assays, such as microparticle-based nucleic acid hybridization assays [12], magnetic bead-based surface-hybridization [13] and hybridization on a DNA microfluidic chip [14]. For expression DNA microarrays, a surface with ssDNA-bound probes is exposed to unknown sample DNA, a technique that can generate great amounts of data [15]. Many technologies have been designed to target and enrich specific regions of genomes to facilitate next-generation sequencing, such as the NimbleGen 385 K Custom Sequence Capture Array [8]. These technologies focus on how to foster more hybridization for downstream results, while we measure actual conformational transformations in order to prevent unwanted hybridization events. Other methods analyze DNA structures based on mobility shifts and UV absorbance changes. SSCP measures the difference in electrophoretic mobilities of mutated DNA fragments analyzed under nondenaturing sieving matrix conditions, for detection of different conformations of ssDNA [16–18]. UV melting analysis detects the change in absorbance when DNA samples are heated, which reflects a conformational change of the DNA [19]. This technique offers the ability to detect melting temperatures of DNA and derive important thermodynamic information. Although these methods are versatile and commonly used in laboratories, we aim to show the method we present in this paper is a cost-effective, simple technique that offers advantages over these techniques.

The work presented here experimentally investigates the dimerization of DNA, as analyzed through free-solution conjugate electrophoresis (FSCE), with the ultimate goal to incorporate experimental results into an algorithm to make predictions for useful barcode primers (the algorithm and software development will be published elsewhere). Advantages in our FSCE method include no polymer sieving matrix to affect mobility with reptation [20], allowing for easily interpreted separations that are low-cost, highly sensitive and quick (under 10 min). However, small dsDNAs (<50 bp) are traditionally not separated well by FSCE, which presents a challenge for the analysis of primer–dimer formation for primer-barcode lengths typically used in sequencing and PCR. Here, we present a way to solve this problem by modifying just one of the two oligos in a primer pair with a polyamide drag-tag [21, 22]. A systematic array of primer barcodes was designed to investigate different forms of double-stranded primer–dimer formation (ds primer–dimers). We chose a primer-barcode length of 30 nucleotides to mimic high multiplexing conditions, where there is greater potential for primer–dimer formation when the barcode misanneals to another adaptor-barcode-primer construct. These barcode cases are analyzed by FSCE at different temperatures, to empirically explore the melting temperatures of different patterns of base-pairing between the primer-barcode mimics. This new mobility shift assay enables separation of short DNA fragments to demonstrate the spatial arrangement of base-pairs are important in primer–dimer formation.

2 Materials and methods

2.1 Reagents and equipment

Tris was obtained from BioRad (Hercules, CA), TAPS from Fisher Scientific (Fairlawn, NJ) and EDTA from Amresco (Solon, OH). PolyDuramide polymer (poly-*N*-hydroxyethylacrylamide, pHEA) (Cambrex BioSciences, Walkersville, MD) was used for dynamic capillary coating, to suppress electroosmotic flow and sample interactions with the internal surface of the capillary [23]. DNA oligomers were purchased from Integrated DNA Technologies (Coralville, IA). Case reactions were annealed using a PTC200 DNA Engine thermocycler (MJ Research, Waltham, MA). Capillary separations were conducted in the ABI 3100 capillary electrophoresis system, consisting of a high-voltage power supply, a 488-nm argon ion laser and a 47-cm length 16-capillary array (36-cm effective length).

2.2 DNA sample preparation

In FSCE, an electrically neutral ''drag-tag'' is conjugated to DNA to add significant hydrodynamic drag in order to break its constant charge-to-friction ratio [22]. Oligomers conjugated to drag-tags were modified at the 5′-end with a thiol linker that has a 6-carbon spacer, and on the 3′-end with rhodamine (ROX) (Supporting Information Table S1). Oligomers tagged with fluorescein (FAM) were modified internally with a fluorescein-dT base. This labeling scheme allowed for two-color LIF detection, which we have previously found to allow the unambiguous assignment of DNA peaks in electropherograms [18, 24].

The drag-tag molecules used in this study are linear *N*-methoxyethylglycines (NMEGs) of length 12, 20, 28 or 36, prepared as described previously [21]. These drag-tags are hydrophilic and water soluble. A sulfosuccinimidyl-4-(*N*-maleimidomethyl)cyclohexane-1-carboxylate (Sulfo-SMCC) moiety is used to covalently link the drag-tag to the thiolated 5′-end of the DNA oligomer. To conjugate drag-tags to different DNA oligos, DNA samples were reduced with a 100:1 molar excess of tris(carboxyethyl)phosphine (TCEP). Reduced DNA oligomers were incubated at room temperature overnight with a 40:1 molar excess of NMEG oligomer.

Drag-tagged DNA oligomers were then directly used in annealing reactions.

For preparation of controls, each DNA oligo was denatured at 95°C for 5 min and snap-cooled on ice for 5 min to maintain ssDNA conformations. For preparation of samples, drag-tagged and non-drag-tagged DNA primers from each case reaction were mixed together, heat-denatured at 95°C for 5 min, annealed at 62°C for 10 min and cooled to 25°C.

2.3 CE

A 16-pM final dilution of each case reaction and control DNA samples were loaded into the capillary array by applying a potential of 1 kV (corresponding to 21 V/cm) for 20 s, and electrophoresed under free-solution conditions (no sieving matrix) by applying a potential of 15 kV (320 V/cm) at various temperatures. The range of temperatures, 18, 25, 40, 55, 62°C, was chosen based on tandem single-strand conformational polymorphism-heteroduplex analysis (SSCP-HA) methods [25, 26]. Because our goal is to develop a method to analyze the proportion of ssDNA to ds primer–dimers, we used 18, 25 and 40°C analysis temperatures to ensure conditions were ideal for single-strand detection. We used temperatures of 55 and 62°C (the upper practical limit of the heating element in the ABI 3100 instrument) in order to also explore temperatures that are conducive to double-strand conformers [16]. The highest electrophoresis temperature, 62°C, also corresponds to the annealing temperature used to react each primer case thermodynamically, and approaches the predicted melting temperatures of individual primers (Supporting Information Table S1).

Each case reaction was electrophoresed at least three times at each temperature and often up to 10 different times to ensure results were reproducible. The running buffer was composed of 1 × TTE (89 mM Tris, 89 mM TAPS, 2 mM EDTA) with 0.03% pHEA added as a dynamic wall-coating agent. Raw LIF data of the T- and A-traces (corresponding to dyes used on oligomers of the case reactions) were converted to text files and processed using ORIGIN (Microcal Software, Northampton, MA). Peaks were subjected to a Gaussian fit using PeakFit (SPSS, Chicago, IL), from which area was estimated under each peak. Areas under double-stranded peaks were divided by total peak area of each electropherogram to calculate the percentage of ds primer–dimer in each case reaction.

2.4 Thermodynamic simulation

The Gibbs free energy (ΔG°) of DNA duplex melting was calculated using AutoDimer [27]. For the calculations, we used temperature, primer concentration, and monovalent salt concentration values as reported above. AutoDimer is based on the nearest neighbor empirical model of nucleotide binding [28].

3 Results and discussion

3.1 Experimental design

Fluorescently labeled oligonucleotide pairs were designed with complementary regions from 5 to 30 base-pairs, to test the extent of primer–dimer formation between 30 nucleotide-long DNA sequences that mimic primers with barcodes used for 454™ sequencing (Fig. 1). Primer–dimer ''cases'' consist of two 30-mer primers, one of which is covalently conjugated to an NMEG drag-tag [21]. The drag-tag changes the mobility of the DNA oligo to distinguish it from the ds primer–dimer and free-draining ssDNA in each case. Case 30 is designed to fully base-pair for an exact complement, and reacts a free-draining non-drag-tagged ''case'' primer (Primer 30) with the drag-tagged common primer (Supporting Information Table S1 and Fig. 1). The ''case'' primers 30, 25, 20, 15 and 5 are named based on how many base-pairs the primer is designed to bind to the common primer. The common primer is used as the template in these case reactions, and provides drag to distinguish the ds primer–dimer from single-stranded free-draining primers. These five case reactions are analogous in their pattern of base-pairing; when complexed in a primer–dimer, base-pairing is consecutive, forming a zipper-like structure with a ''tab'' at the end that consists of mismatched nucleotides (Fig. 1). In contrast, Case 20R and Case 15 V react a free-draining primer with a different drag-tagged common primer to base-pair through every other nucleotide (Case 15 V) or through a random pairing resulting in clusters of two, three and four base-pairs (Case 20R) (Fig. 1). These two cases explore varied base-pairing to account for different types of primer–dimer conformations that can occur between primers of 30 nucleotide lengths.

3.2 Dimerization at low temperature

Control reactions were analyzed for each primer case at each temperature. Figure 2A shows a typical result for control reactions, where the drag-tagged (NMEG-12) common primer is substantially retarded in mobility compared with the non-drag-tagged, free-draining primer used in each case reaction. At 18°C, free-draining primers elute between 7.5–8 min and the drag-tagged common primer elutes approximately one minute after the free-draining primers, allowing for detection of ds primer–dimer formation. For the fully base-paired Case 30, a double-stranded primer–dimer peak elutes between single-stranded primers (Fig. 2B), indicating a shift in mobility of a double-stranded species that has a drag-tag attached to one primer of the primer–dimer. The double-stranded primer–dimer peak is identified in Fig. 2B in two ways: overlapping fluorescence and migration time. Overlapping emission from each dye conjugated to different primers indicates the two primers are migrating together, and therefore have formed a ds primer–dimer. Double-strand primer–dimer formation is

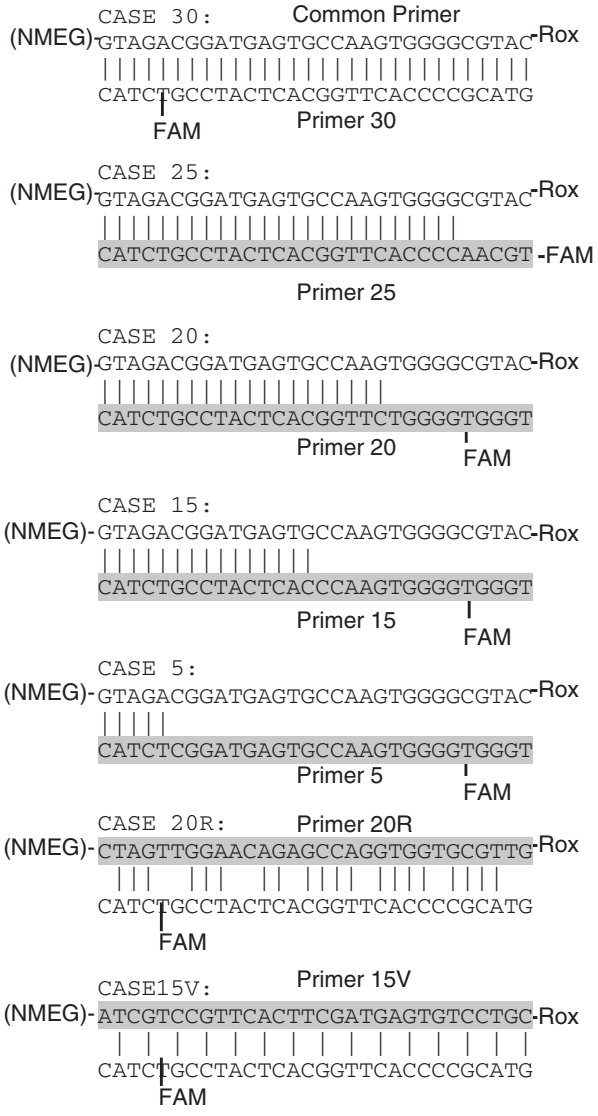

Figure 1. Primer–dimer cases that vary by degree of base-pairing. NMEG denotes the drag-tag molecules used in this study, linear *N*-methoxyethylglycines (NMEGs) of length 12, 20, 28 or 36. Vertical lines connecting primers denote base-pairing. ROX indicates rhodamine dye and FAM signifies fluorescein dye. Shaded oligos are unique to that dimer construct. Oligos with no color are also used in other cases.

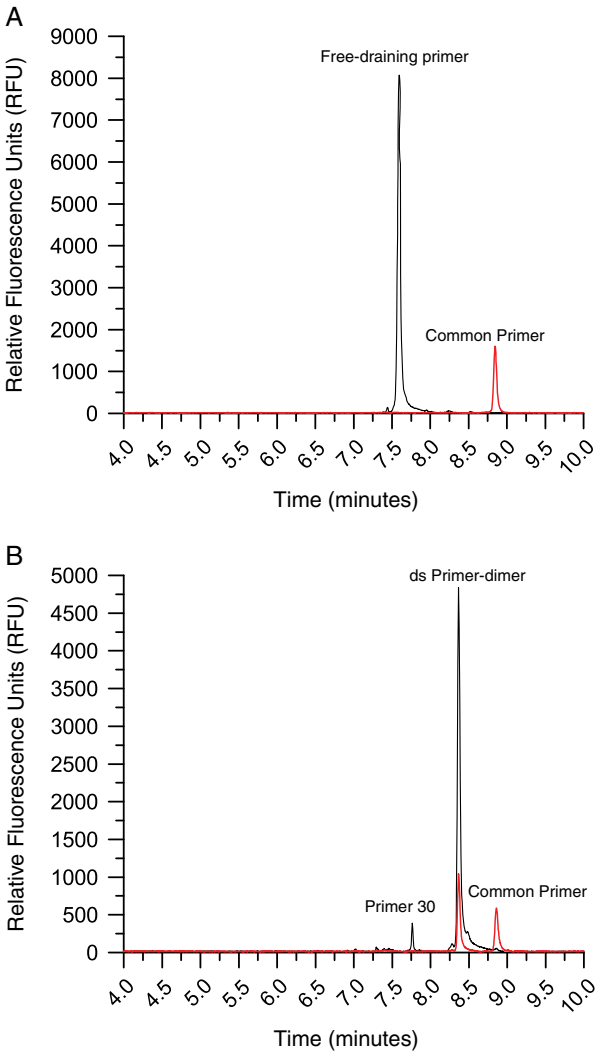

Figure 2. Controls and Case 30 analyzed by CE at 18°C with NMEG-12. (A) Controls run separately and electropherograms overlaid to show differential migration of primers. (B) Case 30 is characterized by fluorescence from two dyes. Red trace corresponds to ROX emission (Common Primer), whereas the black trace corresponds to FAM emission (Primer 30).

further confirmed through elution time, where the primer–dimer elutes in between the free-draining single-stranded Primer 30 and the drag-tagged single-stranded common primer. The primer–dimer migrates faster than the drag-tagged single-stranded common primer since dsDNA migrates faster in free-solution than ssDNA due to doubling of the charge that is associated with increase in molecular weight of the dsDNA [29]. At the same time, the primer–dimer migrates slower than the free-draining single-stranded Primer 30 due to the drag induced by binding a drag-tagged primer. Together, these results demonstrate the ability to accurately and sensitively quantify ds primer–dimer formation by FSCE. The results obtained at 18°C were representative of electrophoretic results for Case 30 when run at 25, 40, 55 and 62°C. Although Case 30 is designed to fully base-pair, the presence of single-stranded primers in the raw data shown in Fig. 2B indicates the reaction is not fully efficient, or reflects slight variance in low sample concentrations, yielding trace amounts of ssDNA.

Cases designed to bind 20 or 25 base-pairs out of the available 30 in the primer–dimer coupling showed different ratios of single-stranded to double-stranded species when separated electrophoretically. A higher relative abundance of single-stranded free-draining primer (Primers 25 and 20, shown in Fig. 3A and B) is present in these case reactions, as compared to the size of the Primer 30 peak in Case 30. Higher amounts of both single-stranded primers in Case 20 (Fig. 3B) indicate that 20 base-pairs is not as efficient at

maintaining a primer–dimer conformation as 25 base-pairs (Case 25) and 30 base-pairs (Case 30). Cases 25 and 20 produce double-stranded primer–dimers: 85% dsDNA for Case 25 (average of 6 runs) and 56% dsDNA for Case 20 (average of 4 runs). These results indicate that a decrease in primer–dimer formation occurs when less base-pairing binds two primers together.

Cases designed to bind their respective binding partner through 15 and 5 base-pairs showed significantly different results from all other cases when separated electrophoretically. Figure 3C and D shows the results obtained at 25°C, which are representative of electrophoretic results for Cases 15 and 5 when run at 18, 25, 40, 55 and 62°C. Lacking is a peak that elutes between the single-stranded primers, or a peak with overlapping fluorescence, indicating no primer–dimer formation. These results suggest that 15 and 5 consecutive base-pairs are not sufficient to strongly bind together a primer–dimer during free-solution electrophoresis, and that the threshold to maintain a primer–dimer within the range of temperatures tested is some value upwards of 15 consecutive base-pairs. Our results indicate that primer constructs with <15 bp dimer-risks should not be able to form significant primer–dimers in the 18–62°C temperature range, and would not be a problem for PCR and 454^{TM} primer design.

To test whether the spatial arrangement of bonds influences the formation of primer–dimers, cases were designed where primer barcodes bind their respective binding partner through 15 and 20 alternating base-pairs (Fig. 1). Figure 4 shows the results obtained at 18°C, which are representative of electrophoretic results for Cases 15 V and 20R when run at 18, 25, 40, 55 and 62°C. Lacking is a peak that elutes between the single-stranded primers, or a peak with overlapping fluorescence, indicating no primer–dimer formation. These results suggest that base-pairing every other nucleotide for a total of 15 base-pairs, and base-pairing in clusters of two, three and four for a total of 20 base-pairs, is not sufficient to strongly bind together a primer–dimer during free-solution electrophoresis. This agrees with previous reports that the ''nearest neighbor'' effects are an important parameter to include for calculating melting temperatures [30].

3.3 Dimerization at high temperature

Above 25°C, ds primer–dimer formation scaled with temperature for Cases 25 and 20. Figure 5 shows the fraction of dsDNA at different temperatures using our FSCE method. At 40°C, Case 25 is not as efficient in maintaining a ds primer–dimer, and Case 20 is even less efficient at maintaining a ds primer–dimer, as fully base-paired Case 30. For Case 25, single-stranded Primer 25 is more abundant than double-stranded primer–dimer indicating a melting event is taking place at 55°C (Supporting Information Fig. S1). At 55°C, melting of the primer–dimer is complete within 20 base-pairs, where both single-stranded primers are present in the electropherogram, without evidence of primer–dimer formation (Supporting Information Fig. S1).

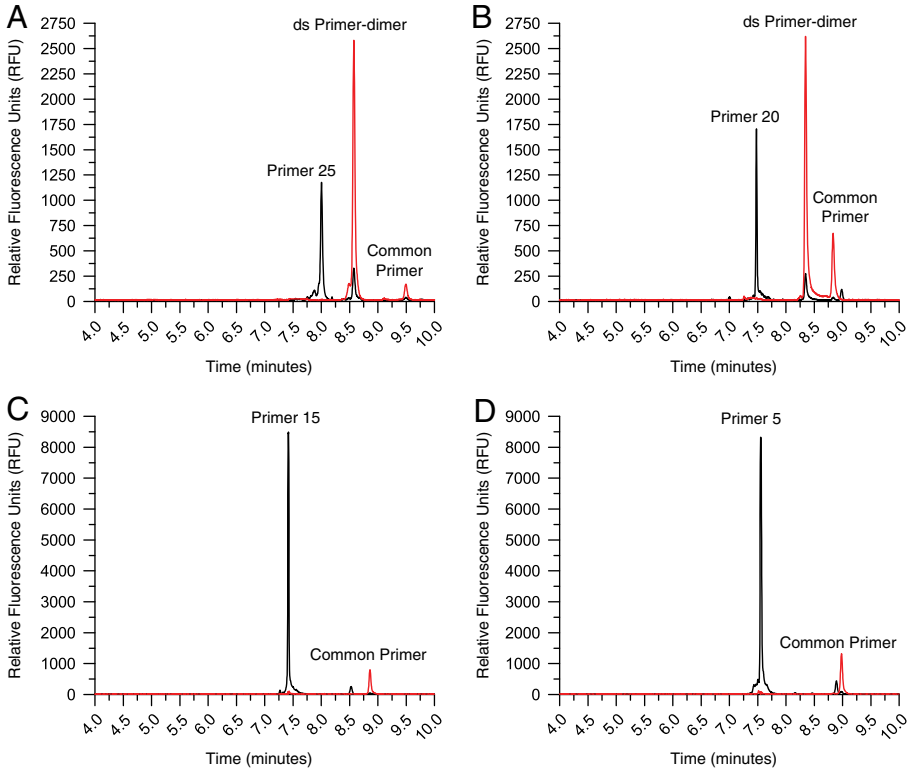

Figure 3. Low-temperature FSCE with NMEG-12. (A) Case 25 shows increased levels of Primer 25 at 18°C. (B) Case 20 has increased levels of single-stranded free-draining primer, Primer 20, at 18°C. (C) Case 15 lacks a ds primer–dimer peak due to insufficient base-pairing at 25°C. (D) Case 5 also lacks double-stranded primer–dimer peaks due to insufficient base-pairing at 25°C.

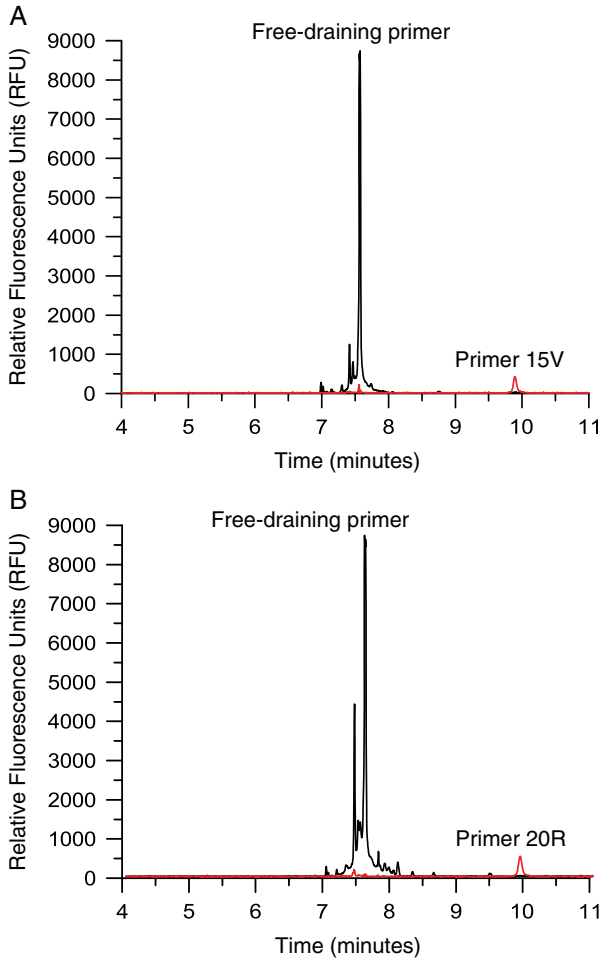

Figure 4. Cases 15 V and 20R analyzed by CE at 18°C with NMEG-28. (A) Case 15V, (B) Case 20R. Both cases lack double-stranded primer–dimer peaks due to insufficient base-pairing.

Full melting of the primer–dimers in Cases 25 and 20 occurs at 62°C. The results shown in Fig. 5 indicate that a temperature between 55–62°C induces a transition that melts the ds primer–dimer formed through 25 base-pairs, as the double-stranded species exists at 55°C, but disappears at 62°C. This is a higher temperature range than for primer–dimers formed from 20 base-pairs, where melting occurs between 40 and 55°C as shown by the presence of a double-stranded species at 40°C, but none at 55°C. Therefore, more base-pairing within a primer–dimer leads to a higher melting temperature of the ds primer–dimer. Also shown in Fig. 5 are the predicted melting temperatures for each case reaction (vertical lines). For Case 20, the fraction of dsDNA vanishes at temperatures above the predicted T_m, validating our results as the theoretical expectation is that dsDNA melts above the T_m. For Case 25, the dsDNA again melted at its predicted T_m, and for Case 30, we could not run the FSCE at the predicted T_m due to instrument constraints. However, the Case 30 ds primer–dimer was stable within 10°C of the predicted T_m.

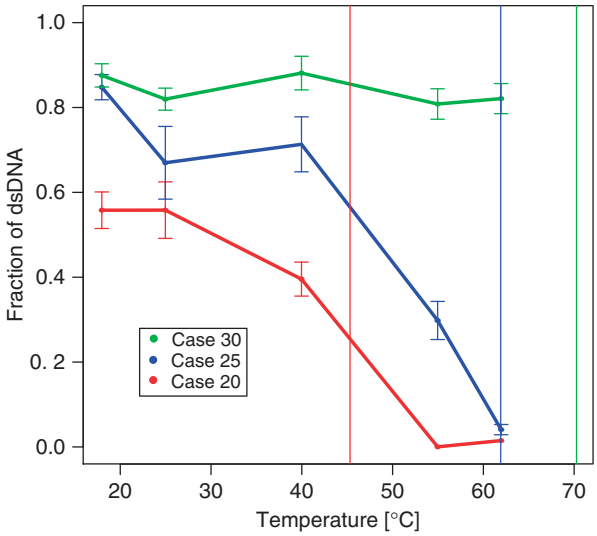

Figure 5. Melting temperature is dependent on degree of base-pairing. Fraction of dsDNA is calculated by comparing area under the peaks of ds primer–dimers to total peak area in each case reaction electropherogram (dsDNA/[dsDNA+ssDNA]). Standard error is shown for $n \geq 3$. The melting temperature (T_m) is indicated by corresponding vertical lines.

Thermodynamics predicts that the energy potential between dsDNA and the two ssDNA that correspond to the DNA duplex, here the ds primer–dimer, is $\Delta G^\circ = \Delta H^\circ - T\Delta S^\circ$. The empirical nearest neighbor model gives the enthalpy and entropy for all dinucleotide bonds [28, 31, 32], thus allowing us to calculate this energy for a particular DNA duplex at a given temperature T (and specified concentrations of the DNA and monovalent salt in solution). Because we are only interested in the relative ratios, we can ignore the partition function. The relative probability of observing dsDNA versus ssDNA is then given by the Boltzmann factor, $P(\Delta G^\circ) = e^{-\Delta G^\circ / k_B T}$, where k_B is the Boltzmann constant. Figure S2, Supporting Information compares theoretical expectations to our observed dsDNA/ssDNA ratio for Cases 20, 25, and 30 at temperatures 18–62°C. Qualitatively, the model prediction and observed dsDNA/ssDNA ratios agree fairly well, and they correlate well (Case 20 $R = 0.86$, Case 25 $R = 0.94$ and Case 30 $R = 0.31$). Quantitatively, however, the prediction was off by orders of magnitudes and the kinetics differed substantially too. Hence, while a simple thermodynamic model can be used to predict T_m and the qualitative behavior of the ds primer–dimers, it cannot accurately predict the quantitative expectation of the amount of dsDNA.

The thermodynamic model we have used assumes that the DNA can only be in two states (dsDNA or ssDNA). While this may seem a gross oversimplification (there are many more states possible in this system), the three peaks corresponding to dsDNA and ssDNA in our system are dominant (Figs. 2–4). The model also assumes that at equilibrium before and after the T_m, the whole population is either dsDNA (at low T) or ssDNA (at high T). As is clear in Fig. 5, this is not the case, i.e. the fraction dsDNA is not 1.0

before we reach T_m. In fact, at $T < T_m$, none of the dsDNA fractions were at unity, suggesting that ssDNA is always present in some fraction. With fewer bonds in the ds primer–dimer, the ssDNA fraction becomes higher. Hence, it is possible that a more complicated thermodynamic model would better predict the observed data.

At higher temperatures, the elution times of both drag-tagged and non-drag-tagged species shortens so that the gap between single-stranded free-draining primers and double-stranded primer–dimers is smaller and more difficult to detect. Due to the input of thermal energy, increased drag is needed to differentiate double-stranded primer–dimers from single-stranded primers. Drag-tags with 20, 28 and 36 *N*-methoxyethylglycines were also explored to counteract short elution times with increased drag. Figure S3, Supporting Information shows the different drag-tags in control reactions at 40°C. At 40°C, free-draining primers elute between 5.5–6 min and the NMEG-12 drag-tagged common primer elutes 30 seconds after the free-draining primer. The NMEG-20, NMEG-28 and NMEG-36 drag-tagged common primers elute approximately 1, 1.5 and 2 min after the free-draining primer at 40°C, respectively. These higher mass drag-tags offer flexibility in this assay and show that a drag-tag that induces more drag can be used for this mobility shift assay at high temperatures.

3.4 Advantages of using FSCE over other DNA hybridization methods

We have found significant advantages in our FSCE method in terms of sample concentration, ease of use, cost, duration of the analysis and sensitivity compared to other DNA binding methods such as hybridization assays, mobility shift assays and UV thermal denaturation techniques. Solid-phase hybridization assays require long hybridization times (ranging from 30 min to 3 days) to hybridize target DNA to surface-bound probes [8, 12, 14]. Sieving matrices also impose limitations on the speed of separation [22], requiring run times between 20 and 25 min of similarly sized oligomers in SSCP and CE [18, 24]. The length of time required for UV thermal denaturation experiments can take as little as 40 min or as long as 3 days if hysteresis is suspected [19, 34]. Our FSCE method presented in this paper hybridizes ssDNA to make ds primer–dimers in solution in 10 min, and achieves small DNA fragment separation in approximately 10 min, to reduce total analysis time and increase throughput, which adds to the cost benefits of using FSCE compared to these techniques.

Our technique is able to detect 16 pM of 30 nucleotide DNA fragments per electrophoretic run, which is over 10 000-fold more sensitive detection than microfluidic hybridization chips [14], microparticle-based hybridization assays [12], other solution-phase hybridization methods [34, 35], SSCP/HA analysis using LPA-based CE [18] and UV melting curves [19, 33]. Our electropherograms show sharp, clearly resolved peaks with high fluorescent signal, allowing for unambiguous evaluation of ds primer–dimer formation. The FSCE method we present in this paper is very sensitive compared these techniques, another factor that boosts the cost-effectiveness of FSCE.

Polymer sieving matrices are difficult to load and increase analysis times [17, 18]. By eliminating the need for polymer sieving matrices in FSCE, we have reduced analysis times and increased ease of use of our method. Viscous polymer sieving matrices are also costly. The cost per run of using a nondenaturing sieving polymer, POP^{TM} Conformational Analysis Polymer (CAP), is approximately $27 (see Supporting Information for calculations). The buffer used for FSCE is prepared in-house and costs approximately $0.02 per run, which is over a 1000-fold cost savings compared to a single run using CAP as a sieving matrix. Only 8 pM of NMEG drag-tag is used in a single case reaction analysis in the method presented here. The NMEG drag-tags are easily synthesized for a relatively modest cost; therefore, the drag-tags themselves represent only a small added expense in FSCE. Electrophoresing primers conjugated to drag-tags in cheap, easy to make buffer instead of commercial sieving polymer makes the cost benefits of using FSCE over gel electrophoresis clear. Overall, the rapid speed of separation and low sample concentrations provide a rapid, low-cost platform for quantifying DNA dimerization using FSCE.

4 Concluding remarks

The results presented here form the basis of a new highly sensitive technique to quantitate primer–dimer formation and separate short, ss and ds DNAs by FSCE. A shift in mobility for double-stranded primer–dimers compared with single-stranded free-draining and drag-tagged primers forms an experimental system that permits rapid and sensitive assessment of primer–dimer formation, incorporating actual 454^{TM}-sequencing and preparative parameters [2]. This platform opens up the potential to use complex and long primer barcodes in massive multiplexing, as problematic non-specific binding can be avoided using certain temperature ranges and ''hot-start'' techniques [10, 36]. Our results indicate primer constructs with <15 bp dimer-risks should not be able to form significant primer–dimers in the 18–62°C temperature range, and would not be a problem for PCR and 454^{TM} primer design. The sensitivity of this technique enables picomolar amounts of primer barcodes to be detected, ensuring that trace amounts of primer–dimers in annealing reactions can be detected. A cutoff for number of consecutive base-pairs necessary to reproducibly bind primer–dimers has been discovered to be higher than 15 of 30 potential base-pairing sites. Bookending the other end of this trend is full complementarity (30 out of 30 nucleotides), which reproducibly binds together primer–dimers even at high temperatures. The temperature at which primer–dimers disassociate is dictated by the number of base-pairs and the pattern of base-pairing formed within a primer–dimer.

Base-pairing across 83% of the primer–dimer (25 out of 30 potential base-pairing sites) decreases the full-complement melting temperature by at least 10°C, whereas base-pairing sequentially across 66% of the heterodimer (20 out of 30 potential base-pairing sites) decreases the full-complement melting temperature by at least 25°C. Cases 20 and 20R illustrated that the spatial arrangement of bonds are important in primer–dimer formation, as primer–dimers formed in Case 20 (sequential base-pairing) but not in Case 20R (staggered base-pairing) even though the same number of base-pairs occurs in each case.

Compared with FSCE, gel technologies, mobility shift assays, other hybridization assays and UV thermal denaturation applications are time-consuming and costly. Electrophoresing primers conjugated to drag-tags in buffer made in-house, instead of a commercial sieving matrix, makes the cost benefits of using FSCE clear. The FSCE method we present in this paper is faster, cheaper and more sensitive than current methodologies typically used to assess the stability of DNA complexes.

Future work will focus on additional case reactions with varied patterns of base-pairing in order to account for different types of primer–dimer conformations that can occur between primers of 30 nucleotide lengths. Specific cases targeting between 15 and 20 base-pairs will probe the cutoff for reproducible primer–dimer formation at a finer scale, in order to define an acute threshold of base-pairing. A more diverse data set will further inform the algorithm for our primer-barcode software, in order to output experimentally optimized primer barcodes for high levels of multiplexing in 454^{TM} sequencing. Although this software will target primer production for 454^{TM} sequencing, the algorithm can easily be adjusted to generate primers for other types of sequencing, barcoding and multiplexing applications, making the results of this study broadly applicable.

This work was supported by National Institutes of Health grant 1 RC2 HG005596-01 as well as a Los Alamos National Laboratory Director's Research grant. The authors thank Prof. Steven Wolinsky and members of his laboratory for help in acquiring primers, and Dr. Jennifer Lin for helpful discussions.

The authors have declared no conflict of interest.

5 References

[1] Wu, X., Xiao, H., *Sci. Chin. C. Life. Sci.* 2009, *52*, 560–567.

[2] Margulies, M., Egholm, M., Altman, W. E., Attiya, S., Bader, J. S., Bemben, L. A., Berka, J., Braverman, M. S., Chen, Y. J., Chen, Z. T., Dewell, S. B., Du, L., Fierro, J. M., Gomes, X. V., Godwin, B. C., He, W., Helgesen, S., Ho, C. H., Irzyk, G. P., Jando, S. C., Alenquer, M. L. I., Jarvie, T. P., Jirage, K. B., Kim, J. B., Knight, J. R., Lanza, J. R., Leamon, J. H., Lefkowitz, S. M., Lei, M., Li, J., Lohman, K. L., Lu, H., Makhijani, V. B., McDade, K. E., McKenna, M. P., Myers, E. W., Nickerson, E., Nobile, J. R., Plant, R., Puc, B. P., Ronan, M. T., Roth, G. T., Sarkis, G. J., Simons, J. F., Simpson, J. W., Srinivasan, M., Tartaro, K. R., Tomasz, A., Vogt, K. A., Volkmer, G. A., Wang, S. H., Wang, Y., Weiner, M. P., Yu, P. G., Begley, R. F., Rothberg, J. M., *Nature* 2005, *437*, 376–380.

[3] Hagan, K. A., Reedy, C. R., Bienvenue, J. M., Dewald, A. H., Landers, J. P., *Analyst* 2011, *136*, 1928–1937.

[4] Fox, S., Filichkin, S., Mockler, T. C., *Methods Mol. Biol.* 2009, *553*, 79–108.

[5] Fischer, W., Ganusov, V. V., Giorgi, E. E., Hraber, P. T., Keele, B. F., Leitner, T., Han, C. S., Gleasner, C. D., Green, L., Lo, C. C., Nag, A., Wallstrom, T. C., Wang, S., McMichael, A. J., Haynes, B. F., Hahn, B. H., Perelson, A. S., Borrow, P., Shaw, G. M., Bhattacharya, T., Korber, B. T., *PLoS One* 2010, *5*, e12303.

[6] Hedskog, C., Mild, M., Jernberg, J., Sherwood, E., Bratt, G., Leitner, T., Lundeberg, J., Andersson, B., Albert, J., *PLoS One* 2010, *5*, e11345.

[7] Tsibris, A. M., Korber, B., Arnaout, R., Russ, C., Lo, C. C., Leitner, T., Gaschen, B., Theiler, J., Paredes, R., Su, Z., Hughes, M. D., Gulick, R. M., Greaves, W., Coakley, E., Flexner, C., Nusbaum, C., Kuritzkes, D. R., *PLoS One* 2009, *4*, e5683.

[8] Hoppman-Chaney, N., Peterson, L. M., Klee, E. W., Middha, S., Courteau, L. K., Ferber, M. J., *Clin. Chem.* 2010, *56*, 1297–1306.

[9] Atrazhev, A., Manage, D. P., Stickel, A. J., Crabtree, H. J., Pilarski, L. M., Acker, J. P., *Anal. Chem.* 2010, *82*, 8079–8087.

[10] Elnifro, E. M., Ashshi, A. M., Cooper, R. J., Klapper, P. E., *Clin. Microbiol. Rev.* 2000, *13*, 559–570.

[11] Nesterova, I. V., Erdem, S. S., Pakhomov, S., Hammer, R. P., Soper, S. A., *J. Am. Chem. Soc.* 2009, *131*, 2432–2433.

[12] Lewis, C. L., Choi, C. H., Lin, Y., Lee, C. S., Yi, H., *Anal. Chem.* 2010, *82*, 5851–5858.

[13] Cai, S., Lau, C., Lu, J., *Anal. Chem.* 2010, *82*, 7178–7184.

[14] Bau, S., Schracke, N., Kranzle, M., Wu, H., Stahler, P., Hoheisel, J., Beier, M., Summerer, D., *Anal. Bioanal. Chem.* 2009, *393*, 171–175.

[15] Venkatasubbarao, S., *Trends Biotechnol.* 2004, *22*, 630–637.

[16] Hestekin, C. N., Jakupciak, J. P., Chiesl, T. N., Kan, C. W., O'Connell, C. D., Barron, A. E., *Electrophoresis* 2006, *27*, 3823–3835.

[17] Kourkine, I. V., Hestekin, C. N., Barron, A. E., *Electrophoresis* 2002, *23*, 1375–1385.

[18] Kourkine, I. V., Hestekin, C. N., Buchholz, B. A., Barron, A. E., *Anal. Chem.* 2002, *74*, 2565–2572.

[19] Mergny, J. L., Lacroix, L., *Oligonucleotides* 2003, *13*, 515–537.

[20] Lerman, L. S., Frisch, H. L., *Biopolymers* 1982, *21*, 995–997.

[21] Haynes, R. D., Meagher, R. J., Won, J. I., Bogdan, F. M., Barron, A. E., *Bioconj. Chem.* 2005, *16*, 929–938.

[22] Meagher, R. J., McCormick, L. C., Haynes, R. D., Won, J. I., Lin, J. S , Slater, G. W., Barron, A. E., *Electrophoresis* 2006, *27*, 1702–1712.

[23] Albarghouthi, M. N., Buchholz, B. A., Huiberts, P. J., Stein, T. M., Barron, A. E., *Electrophoresis* 2002, *23*, 1429–1440.

[24] Kourkine, I. V., Hestekin, C. N., Magnusdottir, S. O., Barron, A. E., *BioTechniques* 2002, *33*, 318–320, 322, 324–325.

[25] Hestekin, C. N., Barron, A. E., *Electrophoresis* 2006, *27*, 3805–3815.

[26] Tian, H., Emrich, C. A., Scherer, J. R., Mathies, R. A., Andersen, P. S., Larsen, L. A., Christiansen, M., *Electrophoresis* 2005, *26*, 1834–1842.

[27] Vallone, P. M., Butler, J. M., *BioTechniques* 2004, *37*, 226–231.

[28] SantaLucia, J., Jr., *Proc. Natl. Acad. Sci. USA* 1998, *95*, 1460–1465.

[29] Nedelcu, S., Meagher, R. J., Barron, A. E., Slater, G. W., *J. Chem. Phys.* 2007, *126*, 175104.

[30] Hughesman, C. B., Turner, R. F. B., Haynes, C., *Biochemistry (NY)* 2011, *50*, 2642–2649.

[31] Breslauer, K. J., Frank, R., Blocker, H., Marky, L. A., *Proc. Natl. Acad. Sci. USA* 1986, *83*, 3746–3750.

[32] SantaLucia, J., Jr., Allawi, H. T., Seneviratne, P. A., *Biochemistry* 1996, *35*, 3555–3562.

[33] Shea, R. G., Ng, P., Bischofberger, N., *Nucleic Acids Res.* 1990, *18*, 4859–4866.

[34] Huber, D. E., Markel, M. L., Pennathur, S., Patel, K. D., *Lab. Chip* 2009, *9*, 2933–2940.

[35] Gnirke, A., Melnikov, A., Maguire, J., Rogov, P., LeProust, E., Brockman, W., Fennell, T., Giannoukos, G., Fisher, S., Russ, C., Gabriel, S., Jaffe, D., Lander, E., Nusbaum, C., *Nat. Biotechnol.* 2009, *27*, 182–189.

[36] Kramer, M. F., Coen, D. M., *Curr. Protoc. Cytom.* 2006, *37*, A.3K.1–A.3K.15.

